Available online at www.sciencedirect.com
ScienceDirect
Corrosion Science 48 (2006) 3513–3530
CORROSION SCIENCE
www.elsevier.com/locate/corsci

Deterioration in critical pitting temperature of 904L stainless steel by addition of sulfate ions

M.H. Moayed [a], R.C. Newman [b,*]

[a] *Materials Engineering Department, Faculty of Engineering, Ferdowsi University, P.O. Box 91775-1111, Mashhad, Iran*
[b] *University of Toronto, Department of Chemical Engineering and Applied Chemistry, 200 College Street, Toronto, Ont., Canada M5S 3E5*

Received 7 March 2005; accepted 22 February 2006
Available online 21 April 2006

Abstract

This paper deals with the effect of adding sulfate on the critical pitting temperature (CPT) of highly alloyed austenitic stainless steel. A large number of potentiodynamic CPT measurements and potentiostatic current–time curves were obtained in 1 M NaCl containing 0, 0.2, 0.5 and 0.75 M Na_2SO_4. Provided the CPT is defined as the first temperature where stable pitting occurs at intermediate potentials, such as 600 mV (Ag/AgCl), addition of sulfate is shown to have the unexpected effect of lowering the CPT. The growing pits formed in sulfate-containing solution passivate anodically as the potential is increased, perhaps via salt precipitation. The effect of sulfate on pitting kinetics was studied using 50 μm-dia. 302SS wire in 1 M NaCl and 1 M NaCl + 0.5 M Na_2SO_4 at 40 °C. Sulfate increases the critical concentration of metal salt in the pit, expressed as a fraction of the saturation concentration, that is required to sustain pit dissolution. Provided this fraction does not exceed 100% of saturation, passivation is enhanced just inside the pit rim, allowing earlier undercutting of the metal surface and a finer pore structure in the lacy metal cover over the pit. The pitting potential measured above the CPT is increased by sulfate addition, but the CPT itself is lowered. Related examples are cited where pitting shows an unusual dependence on some variable such as anion concentration or temperature.

Keywords: A. Stainless steel; C. Pitting corrosion; C. Neutral inhibition

* Corresponding author. Tel.: +1 416 946 0604; fax: +1 416 978 8605.
E-mail address: newman@chem-eng.utoronto.ca (R.C. Newman).

0010-938X/$ - see front matter © 2006 Elsevier Ltd. All rights reserved.
doi:10.1016/j.corsci.2006.02.010

1. Introduction

Localized corrosion of stainless steels is generally believed not to occur in pure sulfate solutions. In practice, when localized corrosion in sulfate solution has been claimed, either the solution was acidic and the procedure unusual, or the steel was a martensitic type with low Cr content. For example, Pickering and Frankenthal [1] induced pits in a Fe–24%Cr alloy exposed to 1 N H_2SO_4 by slowly sweeping the potential from the passive region through the active–passive transition. It is doubtful whether this phenomenon should really be called pitting. On the other hand, the initiation of genuine pitting and crevice corrosion on type 410 martensitic steel in 0.1–1.0 M $Fe_2(SO_4)_3$ (at open-circuit) and in 3 M Na_2SO_4 acidified to pH 2.0 with H_2SO_4 (under potential control), was reported by Mitrovic-Scepanovic and Brigham [2]. They reported similarities between pitting in sulfate and chloride solutions, and showed similar morphology of pits. Since sulfate and chloride are about equally aggressive towards iron, this is a logical result for a low-Cr alloy that is not really a stainless steel.

Pitting corrosion of 300-series stainless steels with much higher Cr contents than 410SS is generally believed to be inhibited by sulfate. On the other hand, by adding controlled concentrations of thiosulfate ions to halide-free neutral sulfate solutions, Garner, Newman and others [3–6] were able to initiate genuine pits in 304SS; this phenomenon used to occur in paper machines. One might say that this should be called thiosulfate pitting, not sulfate pitting, but comparison of chloride and sulfate based systems shows clearly that the pitting is not a separate phenomenon, but a catalysis by thiosulfate of ordinary pitting [7] – in the case of the sulfate solution, activation of anodic metal dissolution is such that the critical pit chemistry can be achieved without chloride.

The normal view of sulfate effects stems from Leckie and Uhlig [8], who reported the inhibitive effect of several anions, including sulfate, perchlorate and nitrate, on pitting corrosion of stainless steels; inhibition was manifested by a positive shift of the pitting potential. They showed that addition of more than 0.15 M Na_2SO_4 to 0.1 M NaCl eliminated pitting at all applied potentials below the potential associated with transpassive dissolution. Nitrate had the ability to inhibit pitting at lower concentrations than sulfate, but only above a certain potential; later this was associated with anodic passivation under a salt film [9], and redox reactions of ferrous ions and nitrate were cited as the reason for this passivation. Ezuber [10] showed using artificial pit electrodes that addition of more than a critical amount of sulfate (an amount that increased with increasing pit depth) induced passivation directly from the salt-covered state, but only *below* a particular potential, in contrast to nitrate; this observation was, and is, unexplained; possibly the ionic constitution of the salt film ($FeCl_2 \cdots FeSO_4$) changes with potential in such a way as to hinder passivation at higher potentials; this may seem the wrong way around, but sulfate is present as bisulfate (HSO_4^-) at low pH, so the double charge of sulfate is not relevant to the argument; analytical data for the salt film are lacking. The effects of dilute sulfate (0.1 M H_2SO_4) on metastable pitting of 304 stainless steel in chloride solution (1 M NaCl) were studied by Pistorius and Burstein [11]. Both initiation and propagation of pitting were inhibited by sulfate. The reduced pit propagation current densities were described quantitatively with respect to the effect of sulfate on the solubility of metal cations (mainly Fe) in the pit anolyte.

This paper is a greatly expanded treatment of a brief note previously published concerning the paradoxical effect of sulfate addition on the critical pitting temperature (CPT) [12].

Insights are included from several publications on the CPT of 904LSS in pure-chloride solutions [13–15].

2. Experimental procedures

2.1. Materials

Type 904L austenitic stainless steel was used for studies of the effect of sulfate addition on temperature-dependent pitting. The 904L alloy contained 20.1 wt.% Cr, 25.0 Ni, 4.32 Mo, 1.41 Mn, balance Fe. It was supplied as plate and machined into rod specimens for most of the pitting experiments.

To measure the rate of pit propagation and to estimate critical pit chemistry in chloride/sulfate solutions, 50 μm-dia. artificial pit (pencil) electrodes made from type 302 stainless steel wire were used. Only a nominal composition was available for this alloy: 17–19 wt.% Cr, 7–11 Ni, balance Fe. 302SS was used because it was available as thin wire; clearly one would not expect its critical pit chemistry for repassivation to be identical to that of 904LSS, but phenomena involving the anodic salt film should not be affected by alloying with Mo, as shown by Laycock who compared 304SS and 316SS [16].

2.2. Specimen preparation

Three types of electrode including artificial pit (pencil) electrodes, plate, and rod, were used in this work. For pencil electrode experiments, the 50 μm 302SS wire was mounted in epoxy resin inside a bent 6 mm glass tube so that one end of the wire was exposed, facing upwards, as the electrode surface. The other end of the wire was connected to a copper wire for electrical connection. The exposed electrode surface was wet ground to 320 grit, using silicon carbide paper, and washed with deionized water prior to each experiment. CPT measurements of 904LSS were carried out using rod ('bullet') electrodes with a waterline, to avoid crevice corrosion. The plate (6 mm) was machined into rods of 4.5 mm diameter and 5 cm length, with one hemispherical rounded end. The other (non-rounded) end of the specimen was connected to the connection wire (nichrome wire) using a screw. These electrodes were mechanically wet ground to 320 grit, washed with deionized water and dried with warm air before use. The immersed length of the specimen was 4 cm, giving a surface area of 4 cm^2. Additionally, 0.3 cm^2 specimens were cut from the plate for exploratory work and for preparation of pits for microscopy. The specimen was welded to nichrome wire for electrical connection. The wire was covered with a heat shrinkable plastic tube for isolation. These specimens were mounted in resin, allowed to set overnight in air, and surface-treated the same way as the rod specimens. The maximum connection resistance was about 1 Ω.

2.3. Electrochemical techniques

All experiments were carried out in NaCl or mixed NaCl/Na_2SO_4 solutions open to air at controlled temperatures, with platinum auxiliary and Ag/AgCl reference electrodes. Analytical grade NaCl and Na_2SO_4, and deionized water, were used throughout. Each experiment used a fresh solution.

An ACM potentiostat (ACM instruments) was used to control the electrode potential. Potential scans were achieved using an ACM sweep generator (ACM instruments) or 16-bit Miniscan (Thompson Electrochem Ltd.). The current between working and auxiliary electrodes was measured either by a digital electrometer in series with the cell or by measuring the voltage across a resistor inserted into the circuit. The analogue output of the electrometer or current output of the potentiostat was connected to an A/D card and the data were stored in a PC.

The potentiodynamic CPT estimation involved the anodic potentiodynamic polarization of the working electrode with a scan rate of 1 mV/s at different temperatures. Before each scan, the working electrodes were left at their open-circuit potential for 5 minutes. Repetitive scans were carried out at different temperatures with 2–3 °C intervals. The surface was refinished after each scan. From the polarization curves, the breakdown potential at which the current increased and remained well beyond the passive current ($>10\ \mu A/cm^2$ sustained for tens of seconds) was determined. The critical pitting temperature was then determined from the plot of the breakdown potential against temperature: there is a narrow range of temperature where a sharp drop in the breakdown potential occurs, from the transpassive region to a value indicative of pitting corrosion. Error bars have not been included on the plots of breakdown potential vs. temperature, but the values indicative of pitting (rather than transpassivity) should be considered valid to ± 20 mV.

The potentiostatic CPT measurement involved applying a constant potential of 750 mV (Ag/AgCl) and ramping the temperature at 0.3 °C/s until stable pitting occurred. Depending on the material and detailed procedure, this has usually been reported to be more reproducible than the repetitive scanning method [14]; however in the present work the exclusive use of the potentiostatic method would have missed the most important feature of the sulfate effect, which occurs at intermediate potentials. Potentiostatic pit current transient measurements were also carried out at appropriate potentials and temperatures.

The artificial pit electrode measurements were carried out in a 250 ml beaker. After initial stabilization of the temperature and open-circuit potential, the specimen was polarized dynamically to 750 mV (vs. Ag/AgCl). This potential is well above the pitting potential of 302SS; formation and coalescence of salt-covered pits led to steady-state diffusion-controlled dissolution. In some experiments the potential was dropped so that the electrode just passed into the active (salt-free) state, then scanned in the positive direction to determine the degree of supersaturation that was possible. Other experiments entailed scanning the potential in the active direction, slowly enough so that the chemistry at the pit surface followed the decreasing current; passivation occurred during these scans and in cases where this was in doubt, the direction of the scan was reversed; if passivation had occurred, it would take time for the former diffusion-controlled condition to be established. The data were used to estimate critical values of the product $D \cdot C$, where D is the diffusivity of the dissolving (Fe, Cr, Ni) cations and C could be the critical dissolved cation concentration to maintain active dissolution (C^*), the saturation concentration (C_s), or the maximum supersaturation concentration (C_{ss}). The ratio of the current density to the limiting current density on the slow back scans was assumed to be equal to the ratio of the dissolved cation concentration at the pit surface to the solubility of the chloride salt; this may involve an approximation, in view of the concentration-dependent diffusivity that is expected in these highly concentrated solutions.

3. Results and discussion

3.1. Effect of sulfate on the CPT (potentiodynamic CPT measurements)

Potentiodynamic CPT estimation for 904LSS in 1 M NaCl revealed a critical pitting temperature of ca. 47 °C for this relatively coarse surface finish (the CPT does depend on surface finish [14]). Fig. 1 illustrates the anodic polarization curves in 1 M NaCl at different temperatures. Previous work had already determined that there is no crevice effect for this kind of bullet specimen [13–15]; microscopic examination confirmed that only genuine pitting was occurring.

Addition of 0.2 M Na_2SO_4 to 1 M NaCl had no significant effect on the CPT using this procedure. These data are summarized in Fig. 2. Comparing with Fig. 1, we can see that this low level of sulfate either has no effect on the CPT or a small beneficial effect; pitting was significantly inhibited around 51 °C. The results obtained at the other sulfate concentrations might suggest that attention should be given to the region around 600 mV in case there are low level but stable pit growth currents, but no conclusive evidence of such effects was found on retrospective examination of the data.

Further CPT measurements revealed that the addition of higher concentrations of sulfate to chloride solution produced a surprising detrimental effect on the CPT. To reach this conclusion, the CPT had to be defined flexibly, not just as the temperature at which pits became unconditionally stable at a very high anodic potential. Sulfate addition produced a current peak in the region of 600–800 mV at temperatures well below the CPT; since the current dropped at higher potentials, one might refer to this as metastable pitting, but for the lower potentials in the pitting range (around 600 mV) there was no evidence that the pitting was repassivating with *time*, only with increasing *potential*. The size of this peak was much larger, and the pitting much more stable, than in the analogous effect reported previously, where metastable pitting peaked at intermediate potentials below the CPT in pure NaCl solution [14]. Here we are clearly dealing with stabilization of pitting by sulfate. A possible reason for the repassivation of pits with increasing potential is salt precipitation

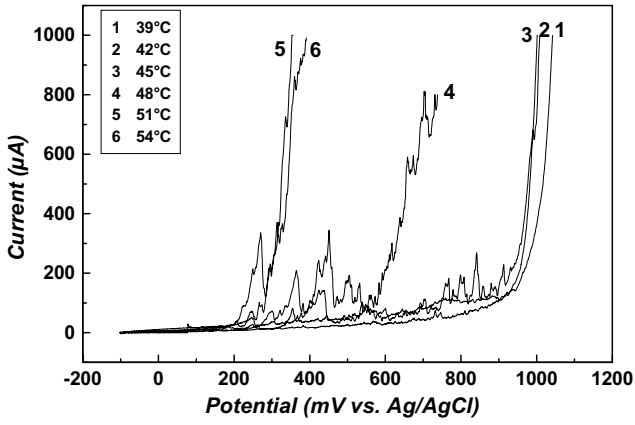

Fig. 1. Anodic polarization curves of 904LSS in 1 M NaCl solution at different temperatures (potential scan rate 1 mV/s).

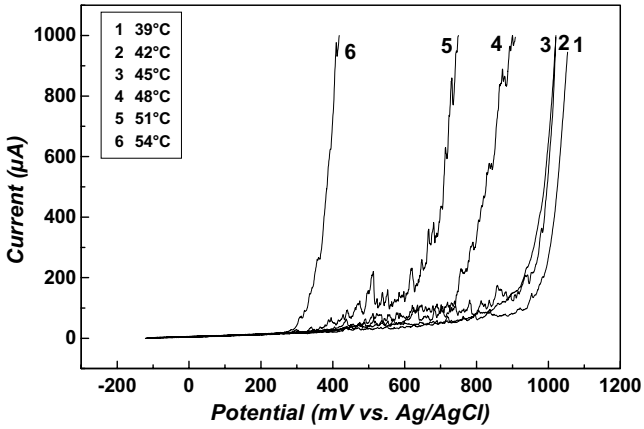

Fig. 2. Anodic polarization curves of 904LSS in 1 M NaCl + 0.2 M Na_2SO_4 solution at different temperatures (potential scan rate 1 mV/s).

and passivation under this salt film, analogous to iron in sulfuric acid [13]; recently a more complex theory has developed, based on undercutting of the metal surface and passivation at the pit rim [15].

Anodic polarization in 1 M NaCl + 0.5 M Na_2SO_4 shows passivity followed by transpassive corrosion at temperatures of 25 and 32 °C (Fig. 3). At 35 °C the hump appears and increases in size up to 41 °C. Finally, at 44 °C, still below the CPT for pure NaCl solution, complete breakdown of passivity occurs at the potential of the hump.

Three to five anodic polarization experiments were carried out at each test temperature to confirm the reality of the current peak due to sulfate, and the general shape of the response was highly reproducible (Fig. 4). These data were taken 9 °C below the CPT that had been estimated for pure NaCl solution (47 °C).

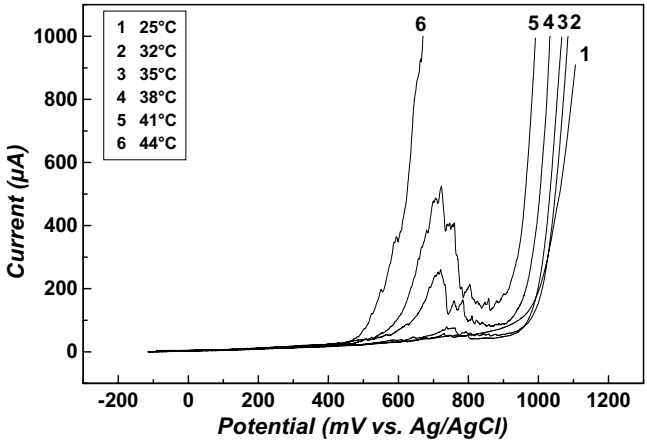

Fig. 3. Anodic polarization curves of 904LSS in 1 M NaCl + 0.5 M Na_2SO_4 solution at different temperatures (potential scan rate 1 mV/s).

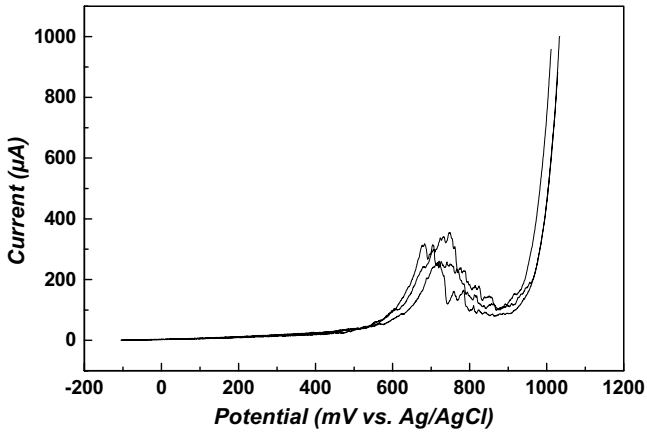

Fig. 4. Three anodic polarization curves of 904LSS in 1 M NaCl + 0.5 M Na_2SO_4 solution at 38 °C (potential scan rate 1 mV/s).

Potentiodynamic polarization curves of 904LSS in 1 M NaCl + 0.75 M Na_2SO_4 at different temperatures are presented in Fig. 5. At temperatures of 25 and 30 °C, the alloy shows passivity followed by transpassive corrosion. As the test temperature increases to 35 °C, a breakthrough followed by a flat current occurs at 550 mV. Increasing the test temperature increases the sharpness of the current rise at 550 mV. Based on this 'hump' region, the CPT for this solution is almost the same as for the 0.5 M sulfate solution, but the pit currents are lower; thus the stabilizing effect of sulfate was less apparent at 0.75 M than at 0.5 M – it appears that there is an optimal sulfate concentration or sulfate to chloride ratio for showing the reduction in the CPT; at very high sulfate concentrations its inhibition tendency would be asserted again.

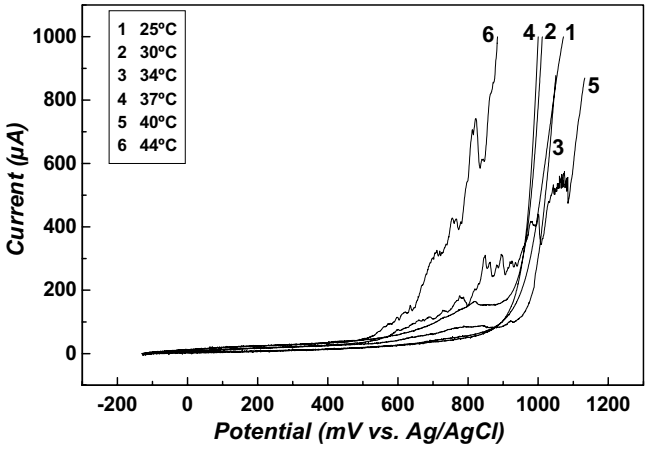

Fig. 5. Anodic polarization curves of 904LSS in 1 M NaCl + 0.75 M Na_2SO_4 solution at different temperatures (potential scan rate 1 mV/s).

3.2. Potentiostatic polarization studies on 904LSS in 1 M NaCl + 0.5 M Na_2SO_4 at 36 and 40 °C

Potentiodynamic polarization curves of 904LSS in 1 M NaCl + 0.5 M Na_2SO_4 show a current hump in the potential range of 520–950 mV with the highest magnitude at around 730 mV (Fig. 4). To explore this effect further, several potentiostatic polarizations were carried out for the same alloy and test solution at 36 °C (11 °C below the CPT estimated for pure-chloride solution) by applying 600, 750, and 920 mV. Fig. 6 illustrates the results of these potentiostatic experiments. When a potential of 600 or 750 mV is applied, the current drops due to growth of the passive film for the first 25 s, then it increases gradually. At 600 mV this increase is continual, but at 750 mV, and especially 920 mV, there is evidence of gradual repassivation. These results are consistent with the presence of the hump in the polarization curve, and confirm that the pitting induced by sulfate should be regarded as stable, since over a certain range of potential the current increases smoothly without any apparent limit.

Potentiostatic data were in accord with the potentiodynamic scans with regard to the effect of temperature. The current transients at different applied potentials at 40 °C were larger than those at 36 °C that were shown in Fig. 6. The highest current was obtained at 750 mV after about 100 s, but then the current gradually decreased (Fig. 7). Again the most stable pitting was at the lowest potential within the hump region, and there was evidence for anodic passivation of the pits.

3.3. Summary of potentiodynamic and potentiostatic results

So far, the data show that sulfate addition promotes stable pitting at intermediate potentials, well below the CPT. Fig. 8 summarizes the breakdown potential as a function of test temperature for potentiodynamic CPT measurements of 904LSS in 1 M NaCl with 0, 0.2, 0.5, and 0.75 M Na_2SO_4. Addition of 0.2 M Na_2SO_4, although it has no significant effect on the CPT, causes an increase of 60 mV in the breakdown potential above the CPT,

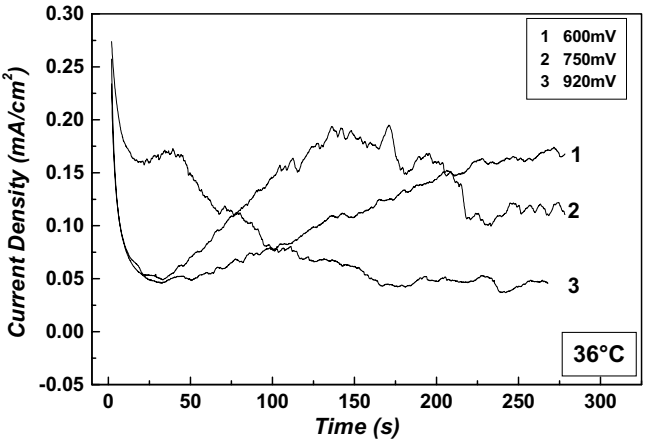

Fig. 6. Current density transients obtained from potentiostatic polarization on 904LSS in 1 M NaCl + 0.5 M Na_2SO_4 solution at 36 °C.

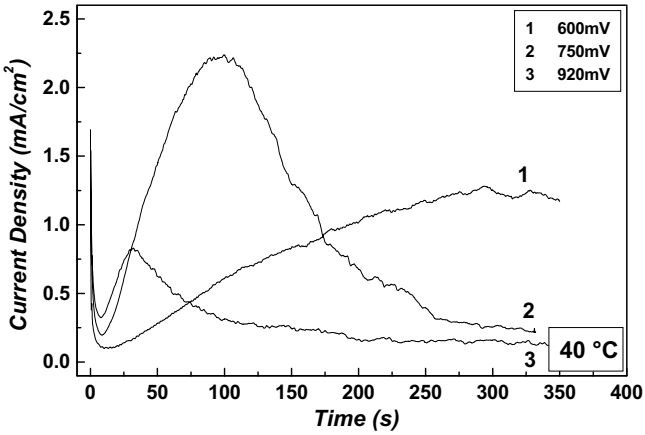

Fig. 7. Current density transients obtained from potentiostatic polarization of 904LSS in 1 M NaCl + 0.5 M Na_2SO_4 solution at 40 °C.

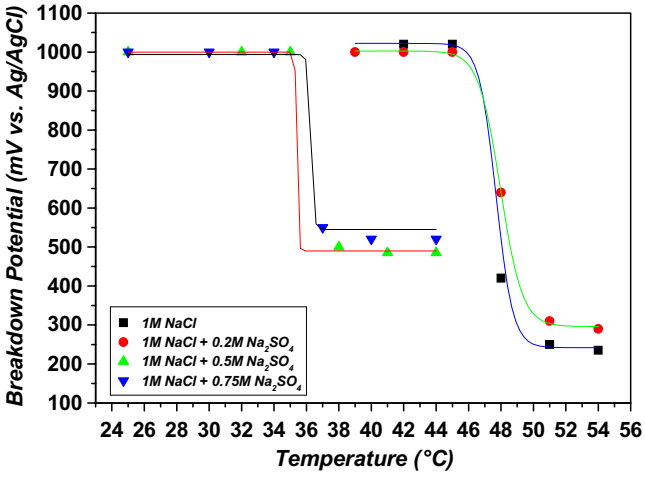

Fig. 8. Plot of breakdown potential vs. test temperature for 904LSS in potentiodynamic polarization experiments.

showing that the normal inhibiting action of sulfate on pitting is present in this region. Further addition of sulfate causes a further increase in the breakdown potential above the CPT, but has a severe detrimental effect on the CPT.

The overall effect of addition of sulfate to 1 M NaCl solution may be summarized as follows:

(1) Inhibitive effect due to shifting the breakdown potential towards the noble direction.
(2) Easier growth of stable pits at lower temperature (reduction in CPT).
(3) Anodic passivation tendency of these stable pits.

Addition of sulfate to chloride solution may affect pitting in the following ways:

(a) Increasing the conductivity of the bulk solution – an increase in the conductivity of the bulk solution will increase the pit growth rate, if pit growth is under partial ohmic control;
(b) Changing the solubility, ionic composition, water content, porosity or other properties of a salt layer over the pit surface, which might promote passivation or alter the effect of beneficial alloying elements like molybdenum;
(c) Changing the critical pit chemistry for stabilization of localized dissolution: generally, sulfate is expected to make passivation easier [10].

The effects of sulfate observed in this work are not unprecedented – they are analogous to the effect of nitrate discussed in the introduction, and to apparently inverted effects of temperature and/or potential on pit stability, discovered by Liew [17] for propagation of artificial pits, and by the present authors [13] for metastable pitting at temperatures below the CPT. Some of these effects, especially those reported by Liew, are known to be related to anodic passivation under a salt film.

It is expected from effect (c) that the tendency of the pit to undercut the surface, producing a lacy metal cover [18,19], will be impacted by the addition of inhibiting anions. This is one promising basis on which to explain the effect of sulfate. When pits are 'stressed' by lowering the temperature or adding an inhibitor, those that grow under the surface, producing a highly occluded geometry, will be favoured. Moreover, such pits may be *more likely to occur* under such borderline conditions. This may lead to an inverted dependence of pit stability on temperature or on the presence of an inhibitor.

3.4. Checking that conductivity is not causing the detrimental effect of sulfate

It needed to be demonstrated that increase in solution conductivity due to addition of sulfate was not causing the observed effects. Potentiostatic CPT and current transient measurements in various chloride-containing solutions were done, whilst altering the solution conductivity by adding extra sodium chloride instead of sulfate, so that the pure-chloride solutions covered the range of conductivities of the mixed solutions. The range of conductivities is shown in Table 1.

For CPT measurements in NaCl solutions of 1.0, 1.3, and 1.5 M, the potentiostatic CPT method using a potential of 750 mV and dynamic heating of the solution was employed as this is more accurate, relatively speaking, than the potentiodynamic method [13–15]; four tests were carried out in each solution. Table 2 illustrates the results.

Table 1
Conductivities of test solutions

Test solution	Conductivity (μS/cm)
1 M NaCl	88,000
1.25 M NaCl	110,000
1.5 M NaCl	125,000
1 M NaCl + 0.2 M Na_2SO_4	110,000
1 M NaCl + 0.5 M Na_2SO_4	116,000
1 M NaCl + 0.75 M Na_2SO_4	124,000

Table 2
Average values and standard deviations of potentiostatic CPT measurements on 904LSS at 750 mV in standard and concentrated chloride solutions

Test solution	No. of specimen tested	Average CPT (°C)	Std. Dev. (°C)
1 M NaCl	4	49.0	0.6
1.3 M NaCl	4	46.9	0.8
1.5 M NaCl	4	46.5	0.9

The effect of increasing conductivity caused by adding extra chloride was much less than the effect of adding sulfate, and there was no current hump when pure-chloride tests were carried out potentiodynamically. The hump is peculiar to the presence of sulfate. Fig. 9 illustrates anodic polarization curves obtained from 904LSS in 1.3 M NaCl and 1 M NaCl + 0.5 M Na_2SO_4 test solutions at 42 °C. The polarization curve in 1.3 M NaCl shows a wide range of passivity with several metastable pits followed by transpassive dissolution. The sulfate-containing solution shows the stable current hump discussed earlier. Potentiostatic tests gave the same conclusion (Fig. 10).

3.5. Exploring the effect of sulfate on the critical pit chemistry

The detrimental effect of addition of sulfate on the CPT is clearly due to other reasons than increasing bulk conductivity. Addition of sulfate into the chloride solution can also change the severity of the pit solution chemistry via migration of SO_4^{2-} anions into the pit, which will act as a buffer via $HSO_4^- = SO_4^{2-} + H^+$ ($pK_a = 1.9$). Sulfate is also incorporated into the anodic salt film [11]. A 50 μm-dia. artificial pit electrode of 302SS was used to explore the effect of sulfate on critical pit chemistry. All the experiments were carried out at 40 °C and initial pit growth was achieved by applying 750 mV (vs. Ag/AgCl) in 1 M NaCl solution, with or without sulfate addition. Only one sulfate concentration was investigated in detail, since we already know [10,19] that there is a monotonic change in the relevant quantities such as solubility of the salt film with sulfate to chloride ratio.

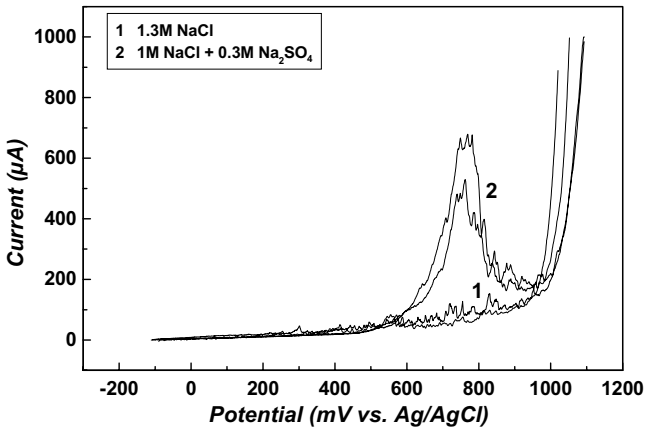

Fig. 9. Anodic polarization curves obtained from duplicate potentiodynamic polarization measurements on 904LSS at 42 °C (potential scan rate 1 mV/s).

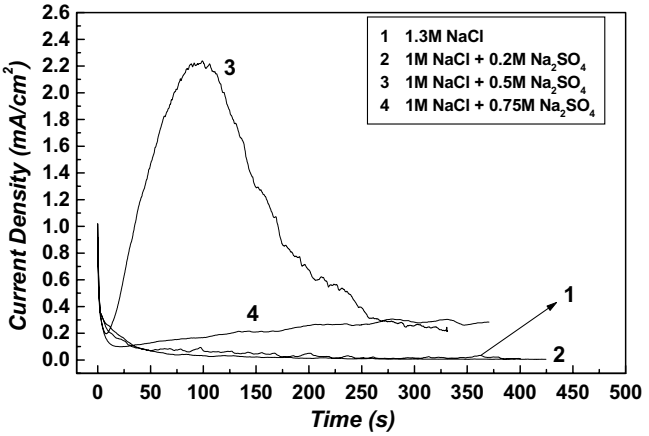

Fig. 10. Current density transients obtained from potentiostatic polarization on 904LSS at 750 mV at 40 °C.

There is no special behaviour of sulfate around 0.5 M so far as kinetics in one-dimensional cavities are concerned – it is only manifested in the more complex 3D geometry of real pits.

3.5.1. Properties of the anodic salt films with and without sulfate

Fig. 11 illustrates current density transients obtained from pencil electrodes of 50 μm 302SS at 750 mV (vs. Ag/AgCl) at 40 °C. After an initial increase of the current density due to formation and coalescence of stable pits, the current density decreases with time, indicating anodic diffusion control in the presence of a salt film. By applying Faraday's second law with an average n value of 2.2 and a metal density of 8.0 g/cm^3 [16], we obtain the pit depth vs. time curves shown in Fig. 12. Good agreement with the expected $i \sim t^{-0.5}$ ($i^2 \sim t^{-1}$) behaviour for anodic diffusion control was confirmed (Fig. 13). Analysis of this figure shows that the $D \cdot C_s$ values for pure-chloride and chloride/sulfate solutions (pro-

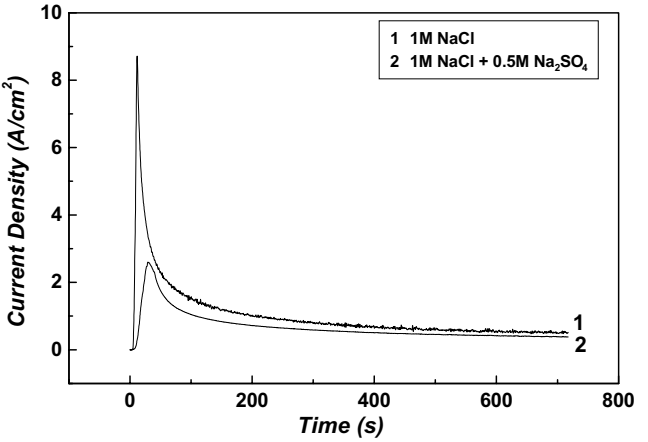

Fig. 11. Potentiostatic current–time curves for 50 μm dia. artificial pits of 302SS at 750 mV (vs. Ag/AgCl) at 40 °C.

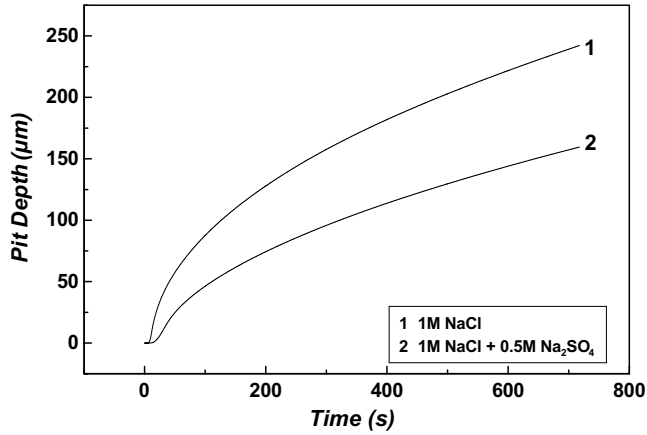

Fig. 12. Pit depth–time curves for 50 μm dia. artificial pits of 302SS at 750 mV (vs. Ag/AgCl) at 40 °C.

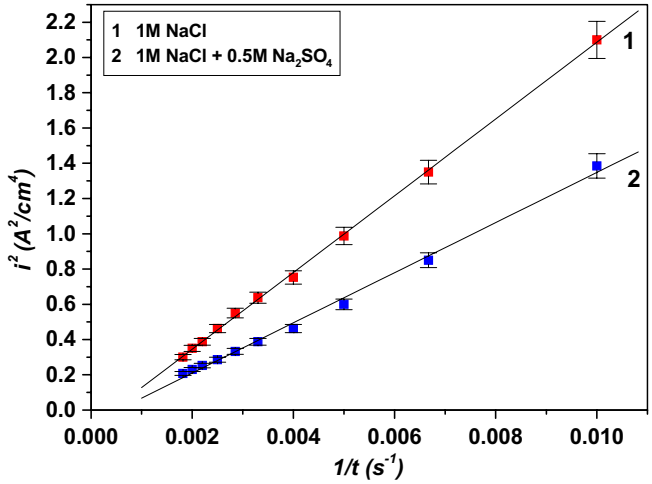

Fig. 13. Plot of i^2 vs. $1/t$ obtained from four i–t curves on growing artificial pits of 50 μm 302SS wire at 750 mV (vs. Ag/AgCl). Test temperature was 40 °C.

portional to the slopes of the lines [16]) are in the ratio $1{:}(0.65 \pm 0.04)$. Assuming that the effect of concentration-dependent diffusivity is small over the applicable range of ionic strengths, this indicates that the solubilities of the anodic salt films formed in these two solutions are approximately in the same ratio. Since the pure-chloride salt is more soluble than the mixed salt, it is reasonable to suppose that there is a slightly lower average or effective cation diffusivity in the pure chloride pits, so the ratio of the solubilities may be slightly larger than the 0.65 calculated.

3.5.2. Supersaturation

Fig. 14 shows the response of the artificial pit to back scanning from the diffusion-controlled condition, followed by forward scanning. The salt film is lost at point a, and

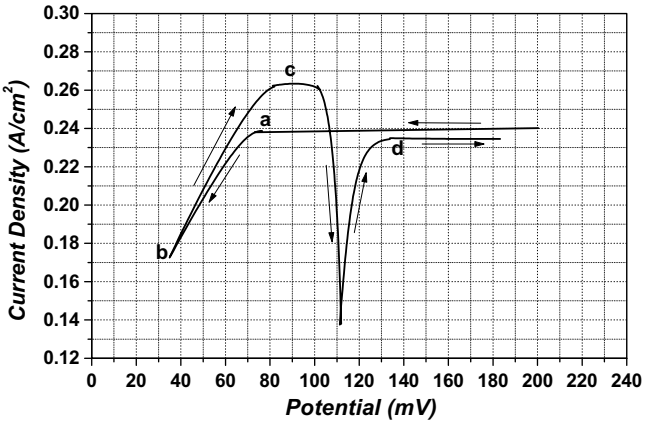

Fig. 14. Presentation of diffusion and activation/IR-drop controlled regimes using a pencil electrode of 50 μm 302SS wire in 1 M NaCl + 0.5 M Na_2SO_4 solution at 40 °C.

ohmic/activation-controlled dissolution ensues. On the subsequent forward scan, provided that passivation has not already initiated at point b, the solution supersaturates (point c), then a thick salt film is precipitated to relieve the supersaturation, producing the deep current minimum; then steady-state diffusion control is re-established (point d). The limiting current is now slightly lower, since the pit has grown slightly during the potential cycle. For several different points 'b' in the ohmic/activation-controlled regime, the potential was scanned in the positive direction and the ratio of i_c/i_d was calculated. This ratio gives an indication of the degree of supersaturation required for precipitation of the salt layer on a salt-free pit surface. This ratio was found to be approximately 1.17 and 1.25 for 1 M NaCl + 0.5 M Na_2SO_4 and 1 M NaCl solutions, respectively. This indicates that precipitation of the (less soluble) salt layer occurs slightly more easily in chloride/sulfate solution than in chloride solution.

3.5.3. Critical pit chemistry for repassivation

Several experiments were carried out with and without sulfate to estimate the critical chemistry C^*, or rather the $D.C^*$ product, for sustaining a pit (C^*: the concentration of dissolved metal salt at the bottom of the pit that is just sufficient to maintain pit growth). Initial diffusion-controlled propagation was done in the usual way, as in Fig. 11, and back scanning was done as in Fig. 14. Successively lower potential limits b were applied until the current response between points b and c shown in Fig. 14 was no longer obtained. If $C > C^*$, i.e. passivation has not initiated, the pit responds by smoothly increasing the current to a higher value than the limiting current density, revealing formation of a supersaturated solution (point c in Fig. 14) as a transitional stage to the saturation concentration that is formed at point d. On the other hand, if passivation has initiated at the negative limit of the scan, a reduced and irregular current response is observed as the pit tries to reactivate itself with increasing potential.

Ideally, one would not need to use this complicated procedure – the current would drop suddenly on the back scan and the critical chemistry would be given by the ratio of the current where this happened to the limiting current. In practice, repassivation of the pit

is quite gradual and dissolution tends to persist, perhaps around the edge of the wire, when most of the pit surface has repassivated; thus we rely for our indication of repassivation on the inability of the pit to regain, immediately, its former state of activity on scanning of the potential in the positive direction.

The values of the critical $D \cdot C$ products are summarized in Fig. 15. The figure displays the 35% lower $D \cdot C_s$ value with sulfate present, already discussed, and shows that this difference does not depend on the pit depth for the pure-chloride system. There may be a slight increase in $D \cdot C_s$ with pit depth for the sulfate system, consistent with the presence of a more complex, mixed salt film; this deserves further investigation. There is, partly as a consequence of the difference in solubility of metal salts, a larger difference between $D \cdot C_s$ and $D \cdot C^*$ values in pure-chloride solution than in the mixed sulfate/chloride solution, indicating more possibility for stable dissolution in the salt-free state in the pure-chloride system. Assuming that D does not vary with concentration, C^*/C_s is about 0.62 in pure chloride and about 0.80 with 0.5 M sulfate added. If there is some concentration-dependent diffusivity, the 0.80 value for the mixed chloride-sulfate system will be more nearly correct than the 0.62 value, on two counts: first, it is a higher ratio, so the range of concentrations is less, and second, the ionic strength of the pit solution is lower in the mixed system. Both ratios fall slightly with increasing pit depth, in line with the expectation that there is a critical current density for passivation at every solution concentration; thus deeper pits, which dissolve more slowly for a given chemistry, will be more tolerant of dilution of the pit anolyte. The ratio C^*/C_s must approach 1, for shallow pits, at the sulfate concentration where complete inhibition of pit initiation is observed at all potentials, which corresponds to a sulfate to chloride ratio of about 1.5 for this temperature.

Since the artificial pit experiments were not done on the 904L alloy, the connection with the natural pitting behaviour is only indirect, but we can expect that the behaviour of 904LSS as a function of sulfate concentration will be similar, especially regarding the values of C_s. Regarding C^*, it appears obvious that this should be higher for the more easily passivated 904LSS than for 302SS at a given temperature, but each alloy will have a range

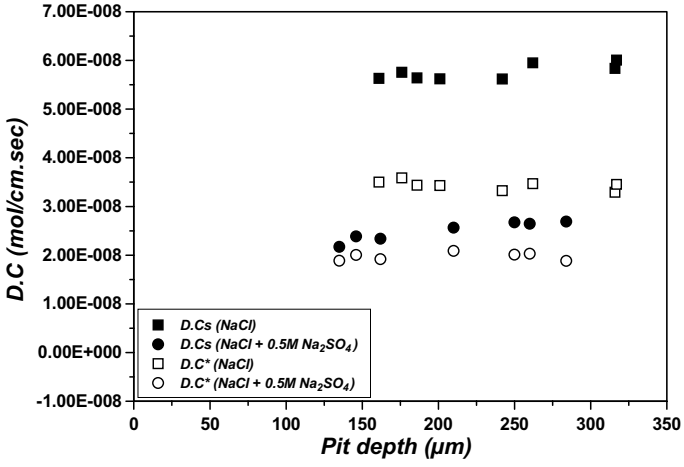

Fig. 15. $D \cdot C_s$ and $D \cdot C^*$ as a function of pit depth for pencil electrodes of 50 μm 302SS in 1 M NaCl and 1 M NaCl + 0.5 M Na_2SO_4 solutions at 40 °C.

of temperatures where analogous behaviour will be seen. The 904L steel is not really a salt-water alloy – it was developed for sulfuric acid service, and its resistance to saline environments is modest. The role of its Cu content in localized corrosion has not been established, but may be detrimental under particular circumstances.

3.6. Shape and stability of corrosion pits in chloride/sulfate solutions

It was shown elsewhere [18,19] that sulfate additions altered the morphology of stable pits in edge-on foil specimens of 304SS polarized in NaCl solutions at room temperature. It was shown that the lacy metal cover over the pit had a finer pore structure when sulfate was added. A similar observation was made on real pits in 904LSS in this work, but instead of being neutral in its effect, the greater occlusion of the pits with sulfate present actually made them more stable and decreased the CPT in this high-alloy material.

The lacy metal cover over a pit forms because passivation occurs near the mouth of a relatively open pit cavity, owing to dilution of the pit solution in that region; then anodic dissolution undercuts the passivated metal and re-emerges at the metal surface; rapid

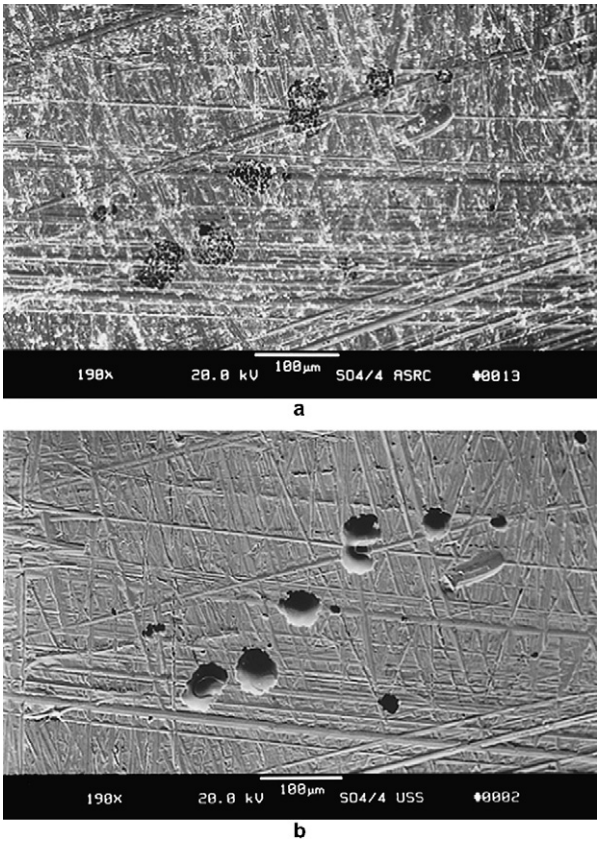

Fig. 16. SEM photomicrographs of stable pits obtained from 904LSS polarized in 1 M NaCl + 0.5 M Na_2SO_4 at 750 mV (vs. Ag/AgCl) and 40 °C : (a) SEM image after the test, (b) SEM image after ultrasonic cleaning.

egress of pit solution from the hole thus created causes further local passivation, and the process repeats itself leading to a passivated lacy metal cover with concentric rings of holes [18–21]. If the value of C^* increases towards, but not quite to, the saturation value C_s, passivation will occur more easily near the pit mouth, and the spacing and size of the holes in the cover will decrease (although initially this is complicated by the fact that with sulfate present, only relatively closed pit cavities can proceed to the stage where they might become stable). So there will be a range of temperatures where, for pure NaCl solution, pits can grow in a fairly stable manner, but even when they undercut the surface, the holes thus produced constitute too open of a geometry to maintain stability against outward diffusion of the pit solution. Addition of moderate sulfate concentrations, by refining the size of the holes without causing undue passivation near the bottom of the pit, stabilizes the pit and lowers the CPT.

These effects are apparent in the SEM micrographs shown above. Fig. 16a illustrates typical pits formed in chloride/sulfate solution at 750 mV (vs. Ag/AgCl) at 40 °C. Pits have different sizes and shapes but are all covered by a lacy cover. When the pit cover was removed by ultrasonic treatment (Fig. 16b), an entirely polished pit surface was revealed, showing that growth occurred under a salt film for a considerable period. Similar images were displayed previously for pure chloride solutions [13–15], but the holes in the

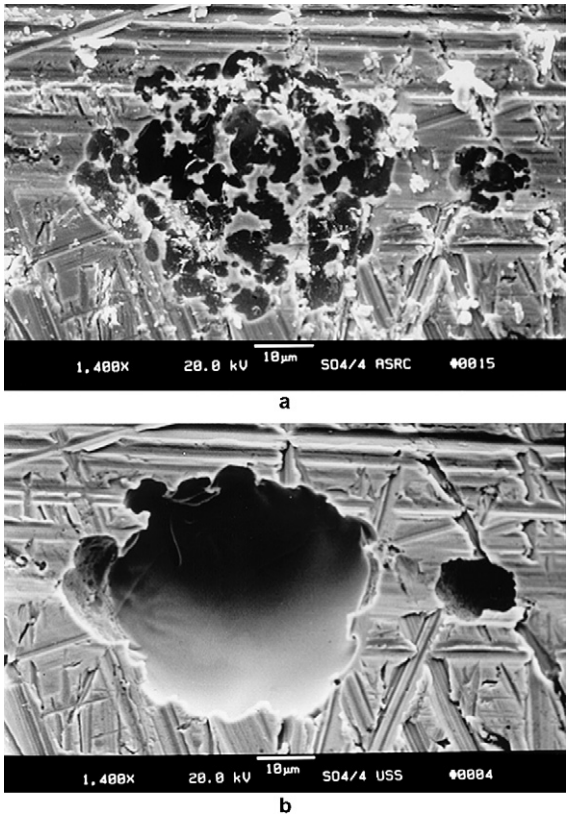

Fig. 17. Higher magnification images of a pit formed in the experiment of Fig. 16.

lacy cover were much coarser; however the present lacy cover morphology does resemble that obtained in chloride/sulfate solutions at room temperature [19].

A higher magnification image is illustrated in Fig. 17. The apparent fraction of empty space in the pit cover is partly an illusion; variation of the accelerating voltage suggested that the cover was more extensive than indicated by these micrographs, and also some material may have been dislodged during preparation. Some regions show evidence of residual passive film over the holes in the lacy cover.

4. Conclusions

Although sulfate is an inhibitor of pitting in stainless steels, expressed in terms of the pitting potential, it can lower the CPT by encouraging pits to grow under the surface. The enhanced pitting with sulfate present occurs over a range of potentials below that normally used for CPT evaluation. The reduction in the CPT can be as much as 12 °C. The lacy metal cover over the pit has a finer pore structure with sulfate present, because passivation is easier in the pit solution (higher ratio of C^* to C_s).

Acknowledgements

The first author wishes to thank the Iran Ferdowsi University of Mashhad for their financial support. We also thank Avesta Polarit for supplying the 904L stainless steel.

References

[1] H.W. Pickering, R.P. Frankenthal, J. Electrochem. Soc. 112 (1965) 761–767.
[2] V. Mitrovic-Scepanovic, R.J. Brigham, Corros. Sci. 27 (1987) 545.
[3] A. Garner, Corrosion 41 (1985) 587.
[4] R.C. Newman, Corrosion 41 (1985) 450.
[5] R.C. Newman, W.P. Wong, A. Garner, Corrosion 42 (1986) 489.
[6] A. Garner, R.C. Newman, W.P. Wong, H. Ezuber, Corrosion 45 (1989) 282.
[7] E.M. Franz, R.C. Newman, Corrosion 40 (1984) 325.
[8] H.P. Leckie, H.H. Uhlig, J. Electrochem. Soc. 113 (1966) 1262.
[9] R.C. Newman, M.A.A. Ajjawi, Corros. Sci. 26 (1986) 1057.
[10] R.C. Newman, H. Ezuber, A.J. Betts, Electrochemical kinetics within localized corrosion cavities, in: B. Elsener (Ed.), Electrochemical Methods in Corrosion Research III, Trans Tech, Zurich, 1989, pp. 247–258.
[11] P.C. Pistorius, G.T. Burstein, Corros. Sci. 33 (1992) 1885.
[12] M.H. Moayed, R.C. Newman, Corros. Sci. 40 (1998) 519.
[13] N.J. Laycock, M.H. Moayed, R.C. Newman, J. Electrochem. Soc. 145 (1998) 2622.
[14] M.H. Moayed, N.J. Laycock, R.C. Newman, Corros. Sci. 45 (2003) 1203.
[15] M.H. Moayed, R.C. Newman, Corros. Sci. 48 (2006) 1004.
[16] N.J. Laycock, R.C. Newman, Corros. Sci. 39 (1997) 1771.
[17] R.C. Newman, K.H. Liew, Corrosion 43 (1987) 58.
[18] P. Ernst, R.C. Newman, Corros. Sci. 44 (2002) 927.
[19] P. Ernst, R.C. Newman, Corros. Sci. 44 (2002) 943.
[20] N.J. Laycock, S.P. White, J.S. Noh, P.T. Wilson, R.C. Newman, J. Electrochem. Soc. 145 (1998) 1101.
[21] N.J. Laycock, S.P. White, J. Electrochem. Soc. 148 (2001) B264.